

Current-constraint speed regulation for PMSM based on port-controlled Hamiltonian realization and deep deterministic policy gradient

Min Wang¹, Yanhong Liu¹, Qi Wang^{1, a)}, and Patrick Wheeler²

Abstract To ensure overcurrent protection, fast dynamic performance and good robustness, a novel speed regulation controller is proposed. The interconnection and damping assignment passivity-based control (IDA-PBC) of Port-controlled Hamiltonian (PCH) systems has the advantages of simple structure and explicit physical meaning. On account of fast dynamic performance and q -axis current-constraint are contradictory, this paper presents a current-constraint speed regulation method for the permanent magnet synchronous motor (PMSM) based on port-controlled Hamiltonian (PCH) realization and deep deterministic policy gradient (DDPG) to balance them. First, a modified IDA-PBC controller with integral action (IA) is constructed, which can regulate the speed and the current of the PMSM simultaneously, and be more suitable for practical applications due to the addition of IA. For both current-constraint and fast dynamic performance, the reinforcement learning of DDPG is utilized to find the optimal parameters of the controller. Finally, experiments are carried out to verify the effectiveness and robustness of the method.

Keywords: current-constraint speed regulation, IDA-PBC with integral action, port-controlled Hamiltonian realization, deep deterministic policy gradient

Classification: Power devices and circuits

1. Introduction

Due to its advantages of high efficiency and high power density [1, 2, 3], PMSMs have been widely used in industrial applications. The PI controller is usually adopted in the speed and current regulation of PMSMs [4]; however, it cannot work well in a large operating region because the controller parameters are generally tuned based on an identified operating condition. With the improvement of processor, intelligent and nonlinear control methods have been gradually introduced, such as fuzzy control [5], neural network control [6], sliding mode control [7] and model predictive control (MPC) [8], have been gradually introduced.

The theory of PCH [9] and the corresponding interconnection and damping assignment passivity-based control (IDA-PBC) [10] have been widely used in industrial applications and process control [11, 12, 13, 14]. For PMSM expressed in Hamiltonian realization, control approaches have been carried out by the IDA-PBC method [15, 16, 17]. The energy characteristics and dissipation structure of the Hamiltonian

system can be used to complete the controller design and stability analysis. It has the advantages of simple structure and explicit physical meaning. However, fast dynamic performance and q -axis current constraint are contradictory [18, 19]. On one hand, fast dynamic performance requires large transient q -axis current to provide a high torque. On the other hand, if conservative constant control parameters are selected for current constraint, dynamic performance will suffer a certain degree of loss. However, maintaining fast dynamic performance under q -axis current constraint is seldom considered in existing PCH-based PMSM control methods.

To enhance the performance of the system, integral action (IA) is always used in the controllers to eliminate static differences, unmatched disturbance and other phenomena ignored by the model assumptions in industrial applications [20, 21]. In [22], the integral action of the IDA-PBC method was added in PCH system (IAPCH) by coordinate transformation and increasing dimensions, and then, a speed regulation controller was designed for the PMSM. However, the damping assignment matrix was not considered in the controller which cannot regulate or even constrain the q -axis current. Moreover, it has not been tested experimentally.

To constrain the current, a PCH with IA controller is designed which can regulate speed and current of PMSM simultaneously and then look for the optimal parameters for both current constraint and fast dynamic performance. Reinforcement learning is a kind of goal-oriented learning method, which aims to find the optimal strategy in time. Lillicrap et al. proposed a deep deterministic policy gradient (DDPG) algorithm [23] based on the framework of the actor-critic method [24]. DDPG has the advantages of taking the high-dimensional state space as the input as deep Q-network (DQN) [25] and solving the high-dimensional continuous action space as deterministic policy gradient (DPG) [26] and has been applied to find optimal parameters [27, 28, 29]. PMSM is a practical application system, and the input and control are continuous, so DDPG is appropriate for application to the PMSM system.

In this paper, we propose a current-constraint speed regulation method based on PCH and DDPG for PMSM. First, the PCH realization of PMSM is present. Second, a speed regulation method which can regulate current based on PCH with IA is proposed. Afterwards, using DDPG to find the optimal parameters, the current-constraint speed regulation controller is obtained. What's more, the closed-loop stability is proved. The experimental results are given finally.

¹ The School of Electrical Engineering, Zhengzhou University, Zhengzhou, China

² The Power Electronics, Machines and Control Group, University of Nottingham, Nottingham, U.K.

^{a)} qwang.cn@outlook.com

The main contributions and novelties of this paper are as follows:

1) This paper presents a PCH-based controller with an integral term that can regulate the speed and the current of the PMSM simultaneously. The additional integral term can increase robustness and guarantee the asymptotic stability of the closed loop system.

2) The DDPG algorithm is utilized to balance q -axis current constraint and fast dynamic performance of the PMSM by seeking the optimal parameters of the PCH-based controller.

3) The proposed controller shows current constraint, good dynamic performance and good robustness against load torque uncertainty. It is verified in experimental results.

2. Hamiltonian realization of PMSM

In this section, we first give the dynamic model of the PMSM and then transform it to its equivalent port-Hamiltonian formulation. The mathematical model of PMSM consists of the electrical dynamics and mechanical dynamic can be described as follows [1, 2, 3]:

$$\begin{cases} L_d \frac{di_d}{dt} = -R_s i_d + n_p \omega L_q i_q + u_d, \\ L_q \frac{di_q}{dt} = -R_s i_q - n_p \omega L_d i_d - n_p \omega \Phi + u_q, \\ J_m \frac{d\omega}{dt} = \tau - \tau_L - B\omega, \end{cases} \quad (1)$$

where L_d , L_q , i_d , i_q , u_d and u_q are d - q axis stator inductances, current, and stator voltage, respectively. R_s is the stator resistance, n_p is the number of pole pairs, ω is the mechanical angular velocity, Φ is the rotor flux linkage, J_m is the inertia, $\tau = \frac{3}{2} n_p [(L_d - L_q) i_d i_q + \Phi i_q]$ is the electromagnetic torque, τ_L is the load torque and B is the viscous friction coefficient. The constraint of the current on the q -axis satisfies $|i_q| < c$, where $c > 0$.

The model of PMSM can be transformed into Hamiltonian realization as follows,

$$\dot{x} = (J(x) - R(x)) \frac{\partial H(x)}{\partial x} + g_u(x)u, \quad (2)$$

the state vector, input vector and the output vector is defined respectively as

$$x = [x_1, x_2, x_3]^T = \left[L_d i_d, L_q i_q, \frac{2}{3} J_m \omega \right]^T, \quad (3)$$

$$u = \left[u_d, u_q, -\frac{2}{3} \tau_L \right]^T, \quad (4)$$

$$y = [i_d, i_q, \omega]^T. \quad (5)$$

The Hamiltonian function is defined as

$$H(x) = \frac{1}{2} (L_d i_d^2 + L_q i_q^2 + \frac{2}{3} J_m \omega^2) = \frac{1}{2} \left(\frac{x_1^2}{L_d} + \frac{x_2^2}{L_q} + \frac{3x_3^2}{2J_m} \right). \quad (6)$$

Then, the model (1) can be represented in the form of a Hamiltonian model with

$$g_u(x) = \begin{bmatrix} 1 & 0 & 0 \\ 0 & 1 & 0 \\ 0 & 0 & 1 \end{bmatrix}, \quad (7)$$

the interconnection matrix is

$$J(x) = \begin{bmatrix} 0 & 0 & n_p x_2 \\ 0 & 0 & -n_p (x_1 + \Phi) \\ -n_p x_2 & n_p (x_1 + \Phi) & 0 \end{bmatrix}, \quad (8)$$

and the damping matrix is

$$R(x) = \begin{bmatrix} R_s & 0 & 0 \\ 0 & R_s & 0 \\ 0 & 0 & \frac{2}{3} B \end{bmatrix}. \quad (9)$$

3. Current-constraint speed regulation for the PMSM based on PCH systems and DDPG

In this section, we first propose a PCH controller based on IDA-PBC with integral action that can regulate the speed and the current of the PMSM simultaneously. Then, the method of finding optimal parameters based on DDPG to balance q -axis current constraint and fast dynamic performance is described. Finally, to obtain i_q^* , a load torque observer is designed to estimate τ_L . The overall diagram of the proposed method is shown in Fig. 1.

3.1 PCH controller based on IDA-PBC with integral action

The full control law, consisting of the input voltages $u = u_r + u_I$, is calculated in two stages, where the regulation term u_r is computed with the IDA-PBC method [10], resulting in the intermediate closed loop dynamics, and u_I is computed the integral action [22], resulting in the final closed-loop system.

The d - q axis reference current and the reference speed are defined as i_d^* , i_q^* , and ω^* , respectively. The constant torque angle control algorithm is utilized for the PMSM drive, where i_d^* is considered to be 0. When the motor reaches the desired equilibrium, one has $d\omega/dt = 0$. Thus, according to (1), i_q^* can be calculated as

$$i_q^* = \frac{2\hat{\tau}_L + 2B\omega^*}{3n_p\Phi}, \quad (10)$$

where the value of $\hat{\tau}_L$ comes from the load torque observer, and the specific design will be represented in subsection 3.3.

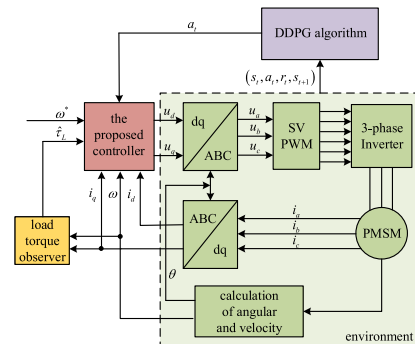


Fig. 1 The overall diagram of the proposed method.

Additionally, the reference state is defined as

$$x^* = [x_1^*, x_2^*, x_3^*]^T = \left[0, \frac{2L_q \hat{\tau}_L + 2L_q B \omega^*}{3n_p \Phi}, \frac{2}{3} J_m \omega^* \right]^T. \quad (11)$$

According to the IDA-PBC technique, a closed-loop energy function $H_d(x)$ with feedback control u_r as constructed to make the PCH system of the PMSM asymptotically stable at the desired equilibrium point x^* , and its minimum value is at x^* . Thus, as described in the following, a feedback controller u_r is constructed such that the intermediate closed loop system is written as

$$\dot{x} = (J_d(x) - R_d(x)) \frac{\partial H_d(x)}{\partial x} + u_I, \quad (12)$$

the PCH controller $u_r = [u_{dr}, u_{qr}, 0]^T$ for the speed control system of PMSM can be derived as

$$\begin{cases} u_{dr} = -r_a i_d - n_p L_d i_q^* (\omega - \omega^*) - n_q L_q i_q \omega^*, \\ u_{qr} = R_s i_q^* - r_b (i_q - i_q^*) + n_p (L_d i_d + \Phi) \omega^*, \end{cases} \quad (13)$$

where r_a and r_b are the parameters of damping assignment matrix. Further, under the controller $u_I = [u_{dI}, u_{qI}, 0, 0]^T$ to add the integral action after the IDA-PBC method, the final closed loop Hamiltonian system is constructed as follows:

$$\dot{z} = \left[\begin{array}{cc|c} J_d(z) & -R_d(z) & 0 \\ \hline 0 & 0 & K_I \end{array} \right] \frac{\partial H_z(z)}{\partial z} \quad (14)$$

with $H_z(z_1, z_2, z_3, z_4) = H_d(z_1, z_2, z_3) + (z_4^T K z_4)/2$, $K > 0$ and

$$\begin{cases} z_1 = x_1, \\ z_2 = x_2 + \frac{L_q}{n_p (L_d i_d + \Phi)} z_4, \\ z_3 = x_3, \\ z_4 = K_I \int (\omega - \omega^*) dt, \end{cases} \quad (15)$$

where K_I is the coefficient of the integral action.

By calculating the integral action controller, the following is constructed:

$$\begin{cases} u_{dI} = 0, \\ u_{qI} = -\frac{L_q K_I (\omega - \omega^*)}{n_p (L_d i_d + \Phi)} + \frac{K_I (-R_s - r_b)}{n_p (L_d i_d + \Phi)} \int (\omega - \omega^*) dt. \end{cases} \quad (16)$$

Theorem 3.1 Consider the PCH system (12) and the control law (16). The closed-loop system can be written as the extended objective PCH (14) with the z -states defined by the state transformation (15). Moreover, the closed-loop system (14) is asymptotically stable at the equilibrium point $(x_1^*, x_2^*, x_3^*, 0)$.

Proof 3.1 Choose $H_z(z)$ as the Lyapunov function of the final closed loop system. Since the reference current comes from the load torque observer, and $i_q^* = \frac{2\hat{\tau}_L + 2B\omega^*}{3n_p\Phi}$. The time derivative of $H_z(z)$ along the trajectory of the final closed loop system is as follows

$$\begin{aligned} \dot{H}_z(z) &= \frac{\partial^T H_z(z)}{\partial z} \left[\begin{array}{cc|c} J_d(z) & -R_d(z) & 0 \\ \hline 0 & 0 & K_I \end{array} \right] \frac{\partial H_z(z)}{\partial z} \\ &= -(R_s + r_a)(i_d - i_d^*)^2 - (R_s + r_b)(i_q - \frac{2\hat{\tau}_L + 2B\omega^*}{3n_p\Phi})^2 \\ &\quad - \frac{2B}{3}(\omega - \omega^*)^2 < 0. \end{aligned} \quad (17)$$

The reference state of z is defined as $z^* = (z_1^*, z_2^*, z_3^*, z_4^*)$. Since $z_4^* = 0$ and the final Hamilton function $H_z(z)$ is constructed based on the intermediate Hamilton function $H_d(x)$, the equilibrium point $z^* = \operatorname{argmin} H_z(z) = (z_1^*, z_2^*, z_3^*, 0)$ corresponds to the numerical values of $(x_1^*, x_2^*, x_3^*, 0)$. The final closed-loop system also preserves the Hamiltonian form, asymptotic stability and equilibrium point as the intermediate Hamiltonian system. This completes the proof.

The final controller u can be obtained as follows:

$$\begin{cases} u_d = -r_a i_d - n_p L_d i_q^* (\omega - \omega^*) - n_q L_q i_q \omega^*, \\ u_q = R_s i_q^* - r_b (i_q - i_q^*) + n_p (L_d i_d + \Phi) \omega^* \\ \quad - \frac{L_q K_I (\omega - \omega^*)}{n_p (L_d i_d + \Phi)} + \frac{K_I (-R_s - r_b)}{n_p (L_d i_d + \Phi)} \int (\omega - \omega^*) dt. \end{cases} \quad (18)$$

With fixed r_b and K_I of controller (18), it is difficult to realize q -axis current constraint and fast dynamic performance of PMSM simultaneously. What's more, it is difficult to accurately obtain the optimal values of the two gains through prior knowledge. We will describe the application of DDPG in the proposed algorithm to find the optimal variables r_b and K_I in the next subsection.

3.2 Method of finding optimal parameters based on DDPG

To constrain the q -axis current and maintain fast dynamic performance, the DDPG algorithm [23] is applicable to find the optimal variables. The overall process of DDPG algorithm of controlling a PMSM system is shown in Fig. 2. The PMSM plays the role of an environment, which provides states to the DDPG algorithm and reacts to an action generated by the algorithm. At each step t , the agent will receive information about states $s_t = (u_d, u_q, i_d, i_q, \omega)_t$ of the PMSM, and the agent will choose an action $a_t = [r_b, K_I]_t$, which influences the current constraint and speed regulation. The DDPG control objective is to maximize the long-term cumulative reward. To obtain the optimal parameters, a multi-objective reward function is created, which is to constrain the q -axis current while maintaining the fast dynamic

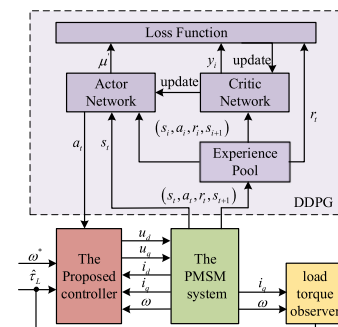


Fig. 2 The algorithm process of DDPG.

performance. The coefficients of each objective of the reward function are based on its importance and magnitude. The reward function $r(s, a)$ is constructed as follows:

$$r(s, a) = \begin{cases} M_i - M_\omega |\omega - \omega^*|, & i_q < c, \\ -M_\omega |\omega - \omega^*|, & i_q \geq c, \end{cases} \quad (19)$$

where $M_i > 0$ and $M_\omega > 0$.

3.3 Load torque observer

When load of torque is constant, to obtain i_q^* , a torque observer is designed to estimate τ_L . The torque observer can be designed as [30, 31]

$$\begin{cases} \dot{\hat{\omega}} = -\frac{B}{J_m} \hat{\omega} - \frac{1}{J_m} \hat{\tau}_L + \frac{1}{J_m} \tau - p_1(\omega - \hat{\omega}), \\ \dot{\hat{\tau}}_L = -p_2(\omega - \hat{\omega}), \end{cases} \quad (20)$$

where $\hat{\omega}$ and $\hat{\tau}_L$ are estimates of ω and τ_L , respectively, and according to pole configuration, the observer gains $p_1 = 2\alpha$, $p_2 = J_m \alpha^2$, and α is the desired bandwidth.

4. Experiments

To verify the effectiveness of the proposed control strategy, an experimental control platform is built to drive a 730W PMSM. The DC bus voltage is 220V. The controller adopts TMS320F28335, and the PMSM is driven by a three-level neutral-point-clamped (NPC) inverter. To test the load disturbance of the proposed method under different conditions, the external load is given by another PMSM with the same power. The experimental platform and parameters of the PMSM are shown in Fig. 3 and Table I, respectively. The parameters in DDPG for our method are shown in Table II, which are determined by the trial and error method and fine-tuned by offline.

There are two types of PMSM experiments, the first type provided a load torque disturbance after the PMSM is powered on, the second type is acceleration. The dynamic performance of the proposed method is compared with IAPCH [8] and PI. In PI, in current loop the parameter is $I = 0.0001$. For comparison, in the speed loop of PI, low-gain parameter $P_1 = 0.009$ is selected to have the current constraint capacity, and high-gain parameter $P_2 = 0.07$ is selected to have the load disturbance ability.

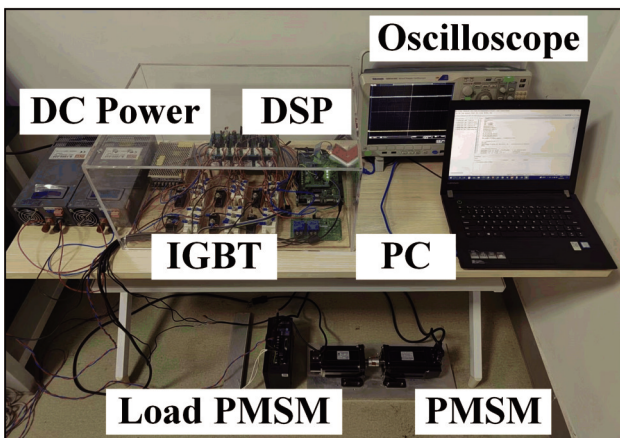


Fig. 3 Photo of the experimental platform.

4.1 Phase of a sudden load torque disturbance

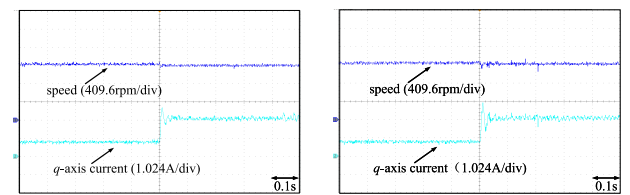
The process of the experiment is adding a load torque suddenly when the PMSM runs at 1250 rpm. Fig. 4(a)–(d) show the performance comparisons of the proposed method, IAPCH, PI with low-gain and PI with high-gain, respectively. There is the shortest recovery time and smallest speed drop under the proposed method compared to IAPCH, high-gain PI and low-gain PI. What's more, the proposed controller has the ability to constrain i_q and better than IAPCH and high-gain PI.

Table I Specifications of the PMSM.

Parameters	Label	Value
rated power	P_{rated}	0.73 kW
rated voltage	V_{rated}	220 V
rated current	I_{rated}	3 A
pole pairs	N_p	4
d-axis inductance	L_d	4.85 mH
q-axis inductance	L_q	4.85 mH
stator resistance	R_s	2.03 Ω
inertia constant	J_m	0.00034 Kg · m ²
rotor flux linkage	Φ	0.13065 Wb

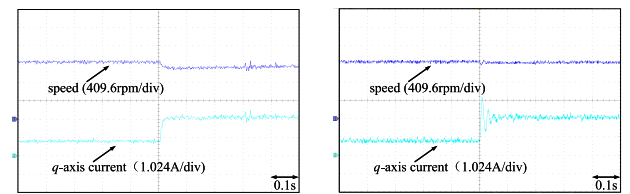
Table II The parameters of the DDPG.

Parameters	Value
layers of Actor	3
layers of Critic	3
number of hidden layer size in Actor	500
number of hidden layer size in Critic	500
Actor learn rate	10^{-5}
Critic learn rate	10^{-4}
Actor gradient threshold	1
Critic gradient threshold	1
experience buffer	10^6
mini-batch size N	64
updating factor ρ	0.01
M_i of reward function	100
M_ω of reward function	0.1
c of reward function	5



(a) Curves under the proposed method

(b) Curves under IAPCH method



(c) Curves under low-gain PI

(d) Curves under high-gain PI

Fig. 4 Performance comparisons.

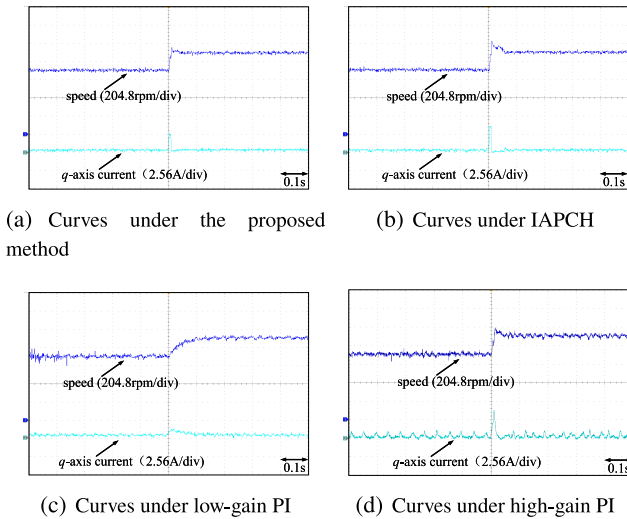


Fig. 5 Performance comparisons (700 rpm to 900 rpm).

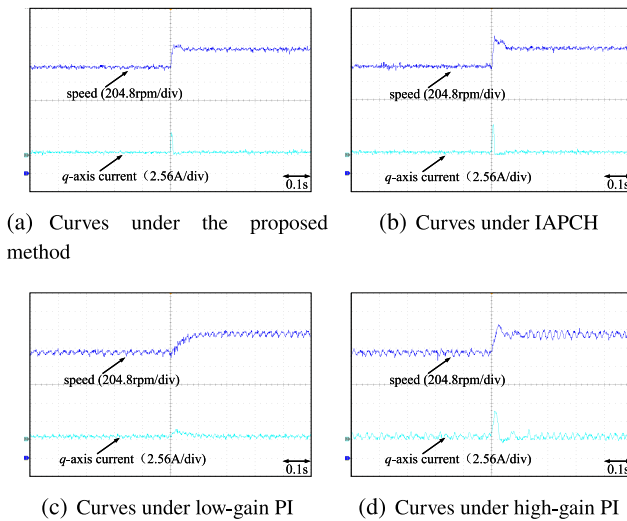


Fig. 6 Performance comparisons (1150 rpm to 1350 rpm).

4.2 Phase of acceleration

There are two experiments about acceleration. The reference speed of the first one is 900 rpm when the PMSM runs at 700 rpm which is shown in Fig. 5. The reference speed of the second one is 1350 rpm when the PMSM runs at 1150 rpm which is shown in Fig. 6. There is the shortest settling time under the proposed method compared to IAPCH, high-gain PI and low-gain PI. What's more, the proposed controller has the ability to constrain i_q and better than IAPCH and high-gain PI.

In conclusion, the proposed method has the ability to simultaneously meet the q -axis current constraint and achieve fast dynamic performance for PMSM.

5. Conclusion

The PCH system of the PMSM views the plant to control from the perspective of overall energy, and the IDA-PBC control method based on the PCH has the advantages of simple structure and explicit physical meaning. However, it cannot balance q -axis current constraint and fast dynamic performance. A PCH-based controller with an integral term

is proposed that can regulate the speed and the current of the PMSM simultaneously. The additional integral term can increase robustness and guarantee the asymptotic stability of the closed loop system. Furthermore, by finding the optimal parameters from the reinforcement learning of DDPG, the proposed method has the ability to balance q -axis current constraint and fast dynamic performance of PMSM. The proposed method shows q -axis current constraint, fast dynamic performance and good robustness.

Acknowledgments

The authors would like to thank the financial support of the National Key Research and Development Project (No. 2020YFB1313701), the National Natural Science Foundation of China (No. 62103376), the Outstanding Foreign Scientist Support Project in Henan Province (No. GZS2019008).

References

- [1] Q. Wang, *et al.*: "A low-complexity optimal switching time-modulated model-predictive control for PMSM with three-level NPC converter," *IEEE Trans. Transp. Electrific.* **6** (2020) 1188 (DOI: 10.1109/TTE.2020.3012352).
- [2] H. Yang, *et al.*: "A loss minimization control method for IPMSM drive system based on improved gradient descent algorithm," *IEICE Electron. Express* **19** (2022) 20220069 (DOI: 10.1587/elex.19.20220069).
- [3] Q. Zeng and Y. Chen: "Sensorless control for PMSM in underwater propeller based on improved phase-locked loop," *IEICE Electron. Express* **18** (2021) 20210111 (DOI: 10.1587/elex.18.20210111).
- [4] W. Wang, *et al.*: "Current harmonic suppression for permanent-magnet synchronous motor based on Chebyshev filter and PI controller," *IEEE Trans. Magn.* **57** (2021) 1 (DOI: 10.1109/TMAG.2020.3017671).
- [5] C. Wang and Z.Q. Zhu: "Fuzzy logic speed control of permanent magnet synchronous machine and feedback voltage ripple reduction in flux-weakening operation region," *IEEE Trans. Ind. Appl.* **56** (2020) 1505 (DOI: 10.1109/TIA.2020.2967673).
- [6] C. Xia, *et al.*: "A neural-network-identifier and fuzzy-controller-based algorithm for dynamic decoupling control of permanent-magnet spherical motor," *IEEE Trans. Ind. Electron.* **57** (2010) 2868 (DOI: 10.1109/TIE.2009.2036030).
- [7] H. Yang, *et al.*: "Generalized super-twisting sliding mode control of permanent magnet synchronous motor based on sinusoidal saturation function," *IEICE Electron. Express* **19** (2022) 20220066 (DOI: 10.1587/elex.19.20220066).
- [8] F. Cai, *et al.*: "Model predictive current control for dual three-phase PMSM with hybrid voltage vector," *IEICE Electron. Express* **19** (2022) 20220340 (DOI: 10.1587/elex.19.20220340).
- [9] A.J. van der Schaft: *L2-Gain and Passivity Techniques in Nonlinear Control* (Springer, London, 2000) (DOI: 10.1007/978-1-4471-0507-7).
- [10] R. Ortega, *et al.*: "Interconnection and damping assignment passivity-based control of port-controlled Hamiltonian systems," *Automatica* **38** (2002) 585 (DOI: 10.1016/S0005-1098(01)00278-3).
- [11] J. Zeng, *et al.*: "An interconnection and damping assignment passivity-based controller for a DC-DC boost converter with a constant power load," *IEEE Trans. Ind. Appl.* **50** (2014) 2314 (DOI: 10.1109/TIA.2013.2290872).
- [12] S. Pang, *et al.*: "Interconnection and damping assignment passivity-based control applied to on-board DC-DC power converter system supplying constant power load," *IEEE Trans. Ind. Appl.* **55** (2019) 6476 (DOI: 10.1109/TIA.2019.2938149).
- [13] T. Zhang and J. Xia: "Interconnection and damping assignment passivity-based impedance control of a compliant assistive robot for physical human-robot interactions," *IEEE Robot. Autom. Lett.* **4** (2019) 538 (DOI: 2019.10.1109/LRA.2019.2891434).

- [14] M.R.J. Harandi and H.D. Taghirad: “Adaptive interconnection and damping assignment passivity-based control for an underactuated cable-driven robot,” *Int. J. Adapt. Control Signal Process.* **35** (2021) 2487 (DOI: [10.1002/acs.3332](https://doi.org/10.1002/acs.3332)).
- [15] M. Khanchoul, *et al.*: “A passivity-based controller under low sampling for speed control of PMSM,” *Control Engineering Practice* **26** (2014) 20 (DOI: [10.1016/j.conengprac.2013.12.013](https://doi.org/10.1016/j.conengprac.2013.12.013)).
- [16] Z. Wu, *et al.*: “Sensorless speed H_{∞} control for PMSM based on energy function,” *Optim. Control Appl. Meth.* **38** (2017) 949 (DOI: [10.1002/oca.2300](https://doi.org/10.1002/oca.2300)).
- [17] M.N. Uddin, *et al.*: “Port controlled Hamilton with dissipation-based speed control of IPMSM drive,” *IEEE Trans. Power Electron.* **35** (2020) 1742 (DOI: [10.1109/TPEL.2019.2918679](https://doi.org/10.1109/TPEL.2019.2918679)).
- [18] T. Guo, *et al.*: “A simple current-constrained controller for permanent-magnet synchronous motor,” *IEEE Trans. Ind. Inf.* **15** (2019) 1486 (DOI: [10.1109/TII.2018.2860968](https://doi.org/10.1109/TII.2018.2860968)).
- [19] Y. Wang, *et al.*: “Speed-current single-loop control with overcurrent protection for PMSM based on time-varying nonlinear disturbance observer,” *IEEE Trans. Ind. Electron.* **69** (2022) 179 (DOI: [10.1109/TIE.2021.3051594](https://doi.org/10.1109/TIE.2021.3051594)).
- [20] A. Larbaoui, *et al.*: “Backstepping control with integral action of PMSM integrated according to the MRAS observer,” *IOSR Journal of Electrical and Electronics Engineering* **9** (2014) 59 (DOI: [10.9790/1676-09415969](https://doi.org/10.9790/1676-09415969)).
- [21] J. Moura, *et al.*: “Online discrete-time LQR controller design with integral action for bulk bucket wheel reclaimer operational processes via action-dependent heuristic dynamic programming,” *ISA Transactions* **90** (2019) 294 (DOI: [10.1016/j.isatra.2019.01.010](https://doi.org/10.1016/j.isatra.2019.01.010)).
- [22] A. Donaire and S. Junco: “On the addition of integral action to port-controlled Hamiltonian systems,” *Automatica* **45** (2009) 1910 (DOI: [10.1016/j.automatica.2009.04.006](https://doi.org/10.1016/j.automatica.2009.04.006)).
- [23] T.P. Lillicrap, *et al.*: “Continuous control with deep reinforcement learning,” *Computer Science* **8** (2015) (DOI: [10.32657/10356/90191](https://doi.org/10.32657/10356/90191)).
- [24] R.S. Sutton and A.G. Barto: *Reinforcement Learning: An Introduction* (MIT Press, Cambridge, 1998).
- [25] M. Volodymyr, *et al.*: “Human-level control through deep reinforcement learning,” *Nature* **518** (2015) 529 (DOI: [10.1038/nature14236](https://doi.org/10.1038/nature14236)).
- [26] S. David, *et al.*: “Deterministic policy gradient algorithms,” 31st International Conference on Machine Learning (2014).
- [27] J. Peng and Y. Yuan: “Moving object grasping method of mechanical arm based on deep deterministic policy gradient and hindsight experience replay,” *Journal of Advanced Computational Intelligence and Intelligent Informatics* **26** (2022) 51 (DOI: [10.20965/jaciii.2022.p0051](https://doi.org/10.20965/jaciii.2022.p0051)).
- [28] Z. Wei, *et al.*: “Deep deterministic policy gradient-DRL enabled multiphysics-constrained fast charging of lithium-ion battery,” *IEEE Trans. Ind. Electron.* **69** (2022) 2588 (DOI: [10.1109/TIE.2021.3070514](https://doi.org/10.1109/TIE.2021.3070514)).
- [29] F. Ying, *et al.*: “Trajectory generation for multiprocess robotic tasks based on nested dual-memory deep deterministic policy gradient,” *IEEE/ASME Trans. Mechatron.* **27** (2022) 4643 (DOI: [10.1109/TMECH.2022.3160605](https://doi.org/10.1109/TMECH.2022.3160605)).
- [30] S.K. Kommuri, *et al.*: “Robust sensors-fault-tolerance with sliding mode estimation and control for PMSM drives,” *IEEE/ASME Trans. Mechatron.* **23** (2018) 17 (DOI: [10.1109/TMECH.2017.2783888](https://doi.org/10.1109/TMECH.2017.2783888)).
- [31] C. Zhu, *et al.*: “Global fast terminal sliding mode control strategy for permanent magnet synchronous motor based on load torque Luenberger observer,” *IEICE Electron. Express* **18** (2021) 20210348 (DOI: [10.1587/elex.18.20210348](https://doi.org/10.1587/elex.18.20210348)).